Frustrated XY models with accidental degeneracy of the ground state

S.E. Korshunov
L.D. Landau Institute for Theoretical Physics, Kosygina 2, 117940 Moscow, Russia

A. Vallat
Department of Physics, Brown University, Providence, Rhode Island, 02912

H. Beck
Institut de Physique, Université de Neuchâtel, Breguêt 1, CH-2000 Neuchâtel, Switzerland
(Received 23 September 1994)

The uniformly frustrated XY model on a triangular lattice is studied for two values of the frustration: $f = 1/4$ and $f = 1/3$. These two cases are very special because the ground states of the model have accidental degeneracy not related to symmetries. This degeneracy originates from the possibility of constructing domain walls with zero energy. At any finite temperature, the accidental degeneracy is removed by the spin-wave free energy, but the low free energy of the domain walls leads to the possibility of phase transitions at temperatures that are much lower than can be expected for the other values of the frustration not leading to accidental degeneracies. These conclusions are supported by Monte Carlo simulations. The results are of relevance for the description of Josephson-junction arrays in the presence of a perpendicular magnetic field.

I. INTRODUCTION

The progress made during the last decade in the experimental investigation of Josephson-junction arrays and superconducting wire networks has led to a revival of interest in various kinds of two-dimentional (2D) XY models which can be applied to the description of such superconducting systems.[1] Of particular interest is the uniformly frustrated XY model which describes regular Josephson-junction arrays in a perpendicular magnetic field. The Hamiltonian of this model can be written as

$$H = -\sum_{\langle \mathbf{r}\mathbf{r}' \rangle} \cos(\theta_{\mathbf{r}} - \theta_{\mathbf{r}'} - A_{\mathbf{r}\mathbf{r}'}), \tag{1}$$

where the summation runs over pairs of nearest neighbors on some regular lattice. The Josephson coupling, the natural unit of energy in the system, has been set equal to 1. For each plaquette (i.e., site of the dual lattice) in a position $\mathbf{R}$ the restriction $\sum_{\Box\mathbf{R}} A_{\mathbf{r}\mathbf{r}'} = 2\pi f$ (where $\sum_{\Box\mathbf{R}}$ means the sum over the bonds surrounding the plaquette $\mathbf{R}$ in a clockwise direction) has to be obeyed. In terms of the Josephson-junction array the variable $\theta_{\mathbf{r}}$ corresponds to the phase of the $\mathbf{r}$th superconducting grain and f to the magnitude of the magnetic field expressed in the number of flux quanta per plaquette. Due to the symmetries of the cosine function Hamiltonian (1) is invariant with respect to the transformations $f \to f \pm 1$ and $f \to -f$, and so it is sufficient to study the interval $f \in [0, 1/2]$.

The main difference between ordinary (f=0) and frustrated XY models is that the ground state in the frustrated model has not only continuous but also descrete degeneracy. For example the f=1/2 model on square or triangular lattices has the Ising-type degeneracy associated with antiferromagnetic ordering of positive and negative vortices.[2] It was also discovered that, for f=1/2 on a hexagonal lattice and f=1/4 on a triangular one, different ground states can exist which are not related to each other by symmetry.[3–6] These ground states can be constructed from each other with the help of zero energy domain walls which are likely to have a strong influence on the properties of the system. The results of Monte Carlo simulations[3] do indeed indicate that both above mentioned cases as well as the f =1/3 (Ref. 5) model on a triangular lattice are characterized by a quite special behavior in comparison with all the other studied cases on these two lattices. Thus these particular systems seem to deserve more attentive consideration.

In the present paper we investigate the properties of the frustrated XY model on a triangular lattice with $f = 1/4$ and $f = 1/3$. Triangular arrays have also been investigated experimentally.[7] We will see that these systems—and in particular the case $f = 1/3$—present a wide family of ground states and zero energy domain walls which should give rise to rather special thermodynamic properties. We hope that our conclusions may also be of relevance for some other frustrated XY models.

II. VORTEX REPRESENTATION

Hamiltonian (1) depends on the choice of gauge variables $A_{\mathbf{r}\mathbf{r}'}$. The same model can be described in terms of gauge-invariant bond variables

$$\phi_{\mathbf{r}\mathbf{r}'} \equiv \theta_{\mathbf{r}} - \theta_{\mathbf{r}'} - A_{\mathbf{r}\mathbf{r}'} + 2\pi n_{\mathbf{r}\mathbf{r}'}, \tag{2}$$

where $n_{\mathbf{r}\mathbf{r}'}$ is the integer for which the value of $\phi_{\mathbf{r}\mathbf{r}'}$ is shifted to the interval $(-\pi, \pi]$. These bond variables have to obey the constraints

$$\sum_{\square\mathbf{R}} \phi_{\mathbf{rr}'} = 2\pi(m_{\mathbf{R}} - f), \tag{3}$$

where $m_{\mathbf{R}} \equiv \sum_{\square\mathbf{R}} n_{\mathbf{rr}'}$ are the integers defined on the dual lattice. The $m_{\mathbf{R}}$'s should not be seen as additional independent variables: They are fully specified once the $\phi_{\mathbf{rr}'}$'s (belonging to a fixed interval of length 2π) are given and on a triangular lattice they can acquire only the values 1, 0 or -1. Hamiltonian (1) can be then rewritten in the form

$$H = -J \sum_{\langle \mathbf{rr} \rangle} \cos \phi_{\mathbf{rr}'},$$

subject to the constraints (3). The symmetries of different ground states can much more easily be recognized in terms of the gauge-invariant variables $\phi_{\mathbf{rr}'}$ (or $m_{\mathbf{R}}$) than in terms of the phase variables $\theta_{\mathbf{r}}$.

We can also define the quantitiy $Q_{\mathbf{R}} \equiv m_{\mathbf{R}} - f$ and interpret it as the topological charge on the corresponding plaquette. The total charge of any state will be equal to zero in the case of periodic boundary conditions. In the ground state the $Q_{\mathbf{R}}$ will acquire only the two different values $1 - f$ and $-f$ when $f \in (-\pi, \pi]$. This charge representation makes it possible to represent different locally stable states of the system (including all the ground states) by the corresponding configuration of the positive topological charges $1 - f$.

III. f=1/4

A. Ground states

For the case $f = 1/4$ the ground state that is depicted in Fig. 1(a) was the first to be discovered.[4] In the following we shall call it the hexagonal ground state. This ground state is characterized by a fourfold discrete degeneracy; i.e., by its translation along the lattice it is possible to obtain four nonequivalent states. It also has the continuous degeneracy associated with simultaneous rotation of all phases, which is not visualized in the charge representation.

The hexagonal state posesses a very interesting feature: For all bonds lying on straight lines that go through the centers of hexagons the gauge-invariant phase differences $\phi_{\mathbf{rr}'}$ are equal to zero. This allows one to construct domain walls with zero energy[6] by choosing one of these lines and shifting the configuration on one of its sides with respect to the other [Fig. 1(b)]. Doing this one obtains another ground state. Any of the three possible directions can be chosen for such a domain wall. However, in order to construct a ground state containing several zero energy domain walls, the latter should be all parallel to each other, because shifting the state along a $\phi_{\mathbf{rr}'}$=0 line breaks the $\phi_{\mathbf{rr}'}$=0 lines in the two other directions.

Nonetheless, an infinite number of states with the same energy can be constructed with the help of such zero energy domain walls. One of them is depicted in Fig. 1(c) (we shall call it the "necklace" ground state). It can be obtained from the hexagonal ground state by creating domain walls on all $\phi_{\mathbf{rr}'}$=0 lines going in the same direction. On the other hand the hexagonal ground state can equally be constructed from the necklace state by creation of an infinite number of zero energy domain walls.

It is well known that accidental degeneracies not related to lattice symmetries can be removed at arbitrary low temperatures due to differences in the spin-wave free energy.[8] So in order to understand what state will be dominant at low temperatures we should compare their spin-wave free energies.

B. Spin-wave free energy

In order to estimate the free energy of the system in the limit of low temperatures it is sufficient to consider the spin-waves in the harmonic approximation. Expanding Hamiltonian (1) up to second order in fluctuations around a ground state configuration $\{\bar{\phi}_{\mathbf{rr}'}\}$ one obtains

$$\begin{aligned} H &= -\sum_{\langle \mathbf{rr}' \rangle} \cos(\bar{\phi}_{\mathbf{rr}'} + \varphi_{\mathbf{r}} - \varphi_{\mathbf{r}'}) \\ &\approx \text{const} + \frac{1}{2} \sum_{\langle \mathbf{rr}' \rangle} K_{\mathbf{rr}'} (\varphi_{\mathbf{r}} - \varphi_{\mathbf{r}'})^2 \\ &\equiv \text{const} + \frac{1}{2} \sum_{\mathbf{rr}'} \varphi_{\mathbf{r}} M_{\mathbf{rr}'} \varphi_{\mathbf{r}'}, \end{aligned} \tag{4}$$

where $K_{\mathbf{rr}'} = J \cos \bar{\phi}_{\mathbf{rr}'}$ and M is the dimensionless dynamical matrix. The $\varphi_{\mathbf{r}}$'s are the deviations of $\theta_{\mathbf{r}}$ from the equilibrium values. The spin-wave free energy per site is given by

$$F_{\text{SW}} = -\frac{T}{N} \ln \sqrt{\frac{(2\pi)^N T^N}{\det M}}, \tag{5}$$

where N is the total number of the sites on the lattice. The zero eigenvalue of M which is related to the rotational invariance of (1) can be removed by fixing the sum of $\varphi_{\mathbf{r}}$ over the whole system.

For periodic ground states the position vector $\mathbf{r}$ can be decomposed into the sum $\mathbf{r} = \mathbf{u} + \mathbf{s}$, where $\mathbf{s}$ denotes the position of a site within an elementary cell of the ground state pattern located at $\mathbf{u}$. The harmonic Hamiltonian (4) can then be expressed in terms of plane waves:

$$H = \frac{1}{2} \sum_{\mathbf{q}ss'} \widetilde{\varphi}_{\mathbf{q}s} M_{ss'}(\mathbf{q}) \widetilde{\varphi}_{-\mathbf{q}s'}, \tag{6}$$

with

$$\widetilde{M}_{ss'}(\mathbf{q}) = \frac{1}{N} \sum_{\mathbf{uu}'} M_{\mathbf{u}+\mathbf{s},\mathbf{u}'+\mathbf{s}'} \exp\left[i\mathbf{q}(\mathbf{u} + \mathbf{s} - \mathbf{u}' - \mathbf{s}')\right]. \tag{7}$$

For example in the hexagonal ground state there are four inequivalent sites within the elementary cell, and so the matrix $\widetilde{M}_{ss'}(\mathbf{q})$ is 4×4. In the limit of a large system we get

$$F_{\rm SW} = \mu T - \frac{T}{2}\ln(2\pi T), \tag{8}$$

where

$$\mu \equiv \frac{1}{2}\int_{\rm BZ}\frac{d^2\mathbf{q}}{(2\pi)^2}\ln\det\widetilde{M}(\mathbf{q}). \tag{9}$$

We have calculated the coefficient μ numerically for five different ground states. In Table I the value of μ is reported as a function of a parameter ν expressing the concentration of the zero energy domain walls (all parallel to each other) on the background of the hexagonal ground state. Here $\nu=1/n$ means that the distance of two consecutive zero energy domain walls is equal to n times the distance between two nearest lines on the lattice; for instance $\nu=1/2$ corresponds to the necklace ground state.

It follows from Table I that the hexagonal ground state has the lowest free energy. It can be also seen that for the other ground states the difference in free energy with respect to the hexagonal one is almost exactly proportional to the concentration of the domain walls ν. One

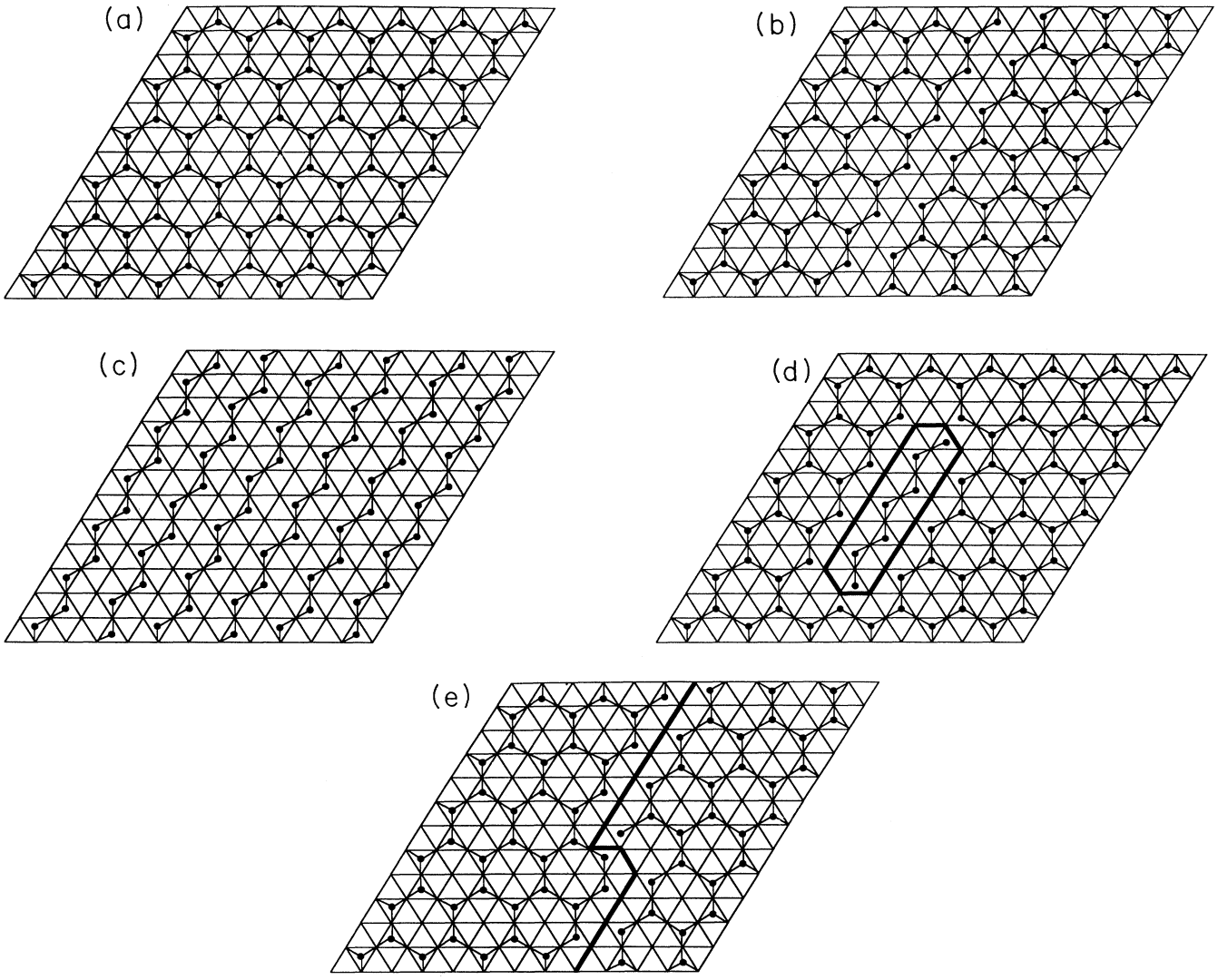

FIG. 1. $f=1/4$. (a) Hexagonal ground state. The values of the $\phi_{\mathbf{r}\mathbf{r}'}$'s are $\pi/2$ on the bonds surrounding a charged plaquette and 0 elsewhere. It is easy to spot the $\phi_{\mathbf{r}\mathbf{r}'}=0$ lines forming a triangular sublattice. The discrete degeneracy of that ground state equals 4. The segments linking the charges are guides to the eye in order to see easily the structure. (b) Ground state with a zero energy domain wall obtained by shifting one half plane of the hexagonal charge configuration along a $\phi_{\mathbf{r}\mathbf{r}'}=0$ line. (c) Necklace ground state obtained from the hexagonal ground state by introducing a maximum number of zero energy domain walls. (d) Low free energy defect or "strip" defect. There are two contributions to the free energy: One comes from the additional spin-wave free energy due to both zero energy domain walls and a second part from the nonzero energy of both defect end points. (e) Single kink. A defect as in Fig. 1(d) can be broadened by double kinks along a zero energy domain wall, but each kink involves an additional energy roughly equal to the one of a defect end point.

TABLE I. $f=1/4$. This table demonstrates the linearity of the spin-wave free energy as a function of the concentration of zero energy domain walls. Here 0 corresponds to the hexagonal ground state, 1/2 to the necklace ground state, and fractional values $\nu=1/n$ to the intermediate periodic ground states in which the distance between the domain walls is n times the distance between two nearest parallel lines on the lattice.

ν	μ	$\Delta\mu \equiv \mu - \mu(0)$	$\gamma \equiv \Delta\mu/\nu$
0	0.37527	0	–
1/8	0.37841	3.14×10^{-3}	2.512×10^{-2}
1/6	0.37948	4.21×10^{-3}	2.526×10^{-2}
1/4	0.38162	6.35×10^{-3}	2.540×10^{-2}
1/2	0.38774	12.47×10^{-3}	2.494×10^{-2}

can certainly interpret these results as evidence for the low interaction between the domain walls and can ascribe to a domain wall the finite free energy per unit length γT with $\gamma \approx 2.5 \times 10^{-2}$.

C. Low-temperature defects and phase transitions

Thus we have obtained that even the maximal difference in free energy for different ground states is very small and decreases with decreasing temperature. A natural question is whether this small difference may lead to any observable consequences. On the one hand a transition to a phase in which the ground state with the lowest spin-wave free energy will be dominant is possible. Alternatively a large concentration of defects leading to a mixture of different states could persist even at arbitrarily low temperatures. If such transition should really occur, at what temperature will it happen?

In order to investigate these questions we start our analysis from the hexagonal ground state which in the harmonic spin-wave approximation has the lowest free energy. This ground state, in addition to a fourfold discrete degeneracy, has also a continuous degeneracy, and so several different possibilities for the phase transitions are open, including the Berezinskii-Kosterlitz-Thouless vortex pair unbinding. At finite temperatures different types of defects on the background of the ground state will be thermally excited, but at low temperatures ($T \ll 1$) the vortices (corresponding either to adding or to substracting 1 to the $Q_{\mathbf{R}}$ of a plaquette from a ground state configuration) will be tightly bound in small pairs, and the energy of domain walls (with the exception of the special zero energy domain walls) will be too large for the corresponding defects to be excited. So the only extended defects that are expected to be present in the system at low temperatures will have the form of a strip enclosed by two zero energy domain walls [Fig. 1(d)].

The free energy of such a defect is equal to

$$F_D(L) = 2E + \alpha T L, \tag{10}$$

where L is the length of the strip (in units of the lattice constant),

$$\alpha = 2\gamma, \tag{11}$$

and $2E$ is the energy of the two end points of this defect. The defects with the minimal value of $E = E_0$ will dominate, and it seems very probable that E is minimal for the minimal distance between the zero energy domain walls [as in Fig. 1(d)]. A numerical evaluation of E_0 gives

$$E_0 \approx 0.44, \tag{12}$$

and the dependence on L would only lead to corrections smaller than 5×10^{-3}.

With the help of Eq. (10) it is easy to estimate the total concentration (per site) of such defects with any size L:

$$c = \frac{(3/m)\sum_{L=1}^{\infty} \exp[-F_D(L)/T]}{1 + (3/m)\sum_{L=1}^{\infty} \exp[-F_D(L)/T]}, \tag{13}$$

where m is the ratio of the total number of sites to the number of possible positions of the defect end points (for $f=1/4$ we have $m=2$). The factor of 3 comes from the summation over three possible directions. Performing the summation gives

$$c = \frac{1}{1 + \frac{m}{3}(e^{\alpha} - 1)\exp[2E_0/T]}, \tag{14}$$

and the average length $\langle L \rangle$ will be equal to

$$\langle L \rangle = \frac{1}{\alpha} + 1. \tag{15}$$

The defects will start touching or crossing each other for $c\langle L \rangle^2 \sim 1$. Since for $f=1/4$ we have $\alpha \approx 0.05$ and $\langle L \rangle \approx 21$ this will happen when the concentration c is much smaller than 1 and can be very well approximated by

$$c \approx \frac{3}{m\alpha} \exp[-2E_0/T]. \tag{16}$$

Comparison with Eq. (15) shows that for $\alpha \ll 1$ the relation $c\langle L \rangle^2 \sim 1$ will be fulfilled at temperatures close to

$$T_* = \frac{2E_0}{3 \ln \frac{1}{\alpha}}. \tag{17}$$

Since α is small, T_* is significantly smaller than 1, and therefore is substantially lower than the critical temperature observed in XY models having a similar rational frustration of the form $f=p/q$ (with $q \leq 5$), but without an accidental degeneracy.

It has to be noted that concentration (14), based on Eq. (10), is evaluated by considering that the striped defects are independent of each other. Whenever two nonparallel defects are crossing each other, we should consider an additional energy that is roughly equal to $4E_0$, and so this effect makes the concentration (14) overestimated. On the other hand, adjacent parallel defects may have a lower free energy than if they were independent. To settle the question whether the latter effect is relevant we consider such a set of defects as a unique defect

but with kinks along its domain walls. Then we must compare the "bare" free energy of the domain wall to its decrease due to the presence of kinks [see Fig. 1(e)].

Let us consider a zero energy domain wall whose spin-wave free energy per unit length is equal to γT. Its free energy decrease due to configurational entropy of the kinks will be equal to

$$\Delta F = T \ln(1 + 2e^{-E_1/T}) \approx 2Te^{-E_1/T}, \tag{18}$$

where E_1 is the energy of the kink. At a temperature $T_{**} \approx E_1/\ln\alpha^{-1}$, the total domain wall free energy $F_{\mathrm{DW}} = \gamma T - \Delta F$ becomes negative. In the vicinity of T_{**} both the number and the size of the defects should increase drastically due to the proliferation of the couples of kinks. So T_{**} yields an other interesting logarithmic estimate for a transition temperature.

We have found numerically that the value of E_1 differs from E_0 only by about 5×10^{-3}. So the direct calculation gives $T_{**} \approx (3/2)T_* > T_*$ and allows one to conclude that in the calculation of T_* the renormalization of α can be neglected. In addition, the comparison of the small difference between E_0 and E_1 with the additional energy due to a crossing of two defects implies that our concentration (14), based on independent simple striped defects, is overestimated. But at temperatures lower than T_* at which the defects are rare the above additional energy can also be neglected. Therefore the value of T_* given by Eq. (17) can be used as an estimate for the lower bound of a transition temperature, because there is no reason for a phase transition to take place when all defects are well localized and far from each other.

At temperatures higher than T_* the strip defects start merging with each other and the domain wall free energy rapidly tends to zero; so we have to expect the disappearance of the discrete order associated with the dominance of one of the four equivalent hexagonal ground states. This may happen as a first-order or a second-order phase transition. Since typical defects at low temperatures are very anisotropic and their crossing costs a relatively high energy one may think also of a possibility of the existence in some intermediate range of temperatures of the phase in which only noncrossing (i.e., parallel on the average) infinite domain walls are present. In this phase only two of the four possible hexagonal states will be intermixed (depending on the orientation of the infinite domain walls). Thus the transition associated with destruction of the discrete order may be split into two.

The other kind of ordering present in the system, that is, the XY-type ordering characterized by a finite rigidity (i.e., a finite helicity modulus), is not necessarily destroyed simultaneously with discrete ordering. From the structure of the zero energy domain walls it can be seen that they do not help to make a twist between two opposite sides of the system, and so the continuous degrees of freedom do not feel their presence directly and interact only with kinks and corners on the domain walls. The thermal fluctuations will lead to a decrease of the helicity modulus not only due to the presence of the strip defect end points and nonzero energy domain walls which affect locally the rigidity, but also due to presence of vortex pairs formed by the ordinary (integer) vortices or the fractional vortices which can be associated with corners on the domain walls.[6]

In the general situation the destruction of XY-type ordering is usually driven by the decoupling of (integer or fractional) vortex pairs, and the fractional vortices (if they can move around) are most dangerous since their interaction energy is the lowest.[6] In the present system, however, the fractional vortices are always linked by a domain wall with nonzero energy, and so in the vicinity of the temperature T_*, which is logarithmically small, all the effects leading to the decrease of the helicity modulus (including the presence of any kind of vortex pairs) can be expected to be not important. Therefore it looks more probable that the destruction of the XY-type ordering will take place as a separate phase transition at the temperature which is higher than T_*. It may be either a transition with a universal or higher than universal jump of the helicity modulus depending on what kind of vortex pairs will be dominant at the transition.

On the other hand it cannot be altogether excluded that the cumulative effect of all the mechanisms involved in the decrease of the helicity modulus in the vicinity of T_* (which is only logarithmically small) might be be sufficient to make that decrease important. In that case the simultaneous destruction of both types of ordering may happen which would be accompanied by a nonuniversal jump. One has to bear in mind, however, that in that case the destruction of the XY-type ordering may become observable only at the scales which are much larger than the typical size of the strip defect. In any case the presence of the large quantity of strip defects should lead to a significant decrease of the helicity modulus in comparison to the systems without accidental degeneracy.

IV. $f=\frac{1}{3}$

A. Ground states

The case of $f = 1/3$ demonstrates even a larger variety of ground states than $f=1/4$. One can again start from the ground state with hexagonal symmetry [Fig. 2(a)]. This is the one which is observed in Monte Carlo simulations and was recognized in Ref. 5. This state has a ninefold degeneracy. Just as in the case $f = 1/4$ the gauge-invariant phase differences $\phi_{\mathbf{rr}'}$ on the lines that go through the centers of hexagons are equal to zero, and so again the zero energy domain walls can be constructed [Fig. 2(b)]. However, in contrast to the case of $f=1/4$, a shift of a half plane of a ground state configuration along such a line can lead to two different configurations depending on the sign of the translation vector determining the shift [note the difference between the two zero energy domain walls in Fig. 2(b)]. As in the case of $f = 1/4$ it turns out to be possible to have an arbitrary number of such domain walls with the same orientation without any change in the total energy. If the domain walls are introduced on every possible position (and with the same direction of the shift), the ground state depicted

in Fig. 2(c) is obtained (the necklace ground state).

In all the ground states considered in this section the gauge-invariant bond variables $\phi_{\mathbf{r}\mathbf{r}'}$ are determined by the following rules:

(a) Each charged plaquette (i.e., the plaquette with $Q_{\mathbf{R}}=2/3$ or $m_{\mathbf{R}}=1$) is surrounded by three bonds on two of which $\phi_{\mathbf{r}\mathbf{r}'}$ (counted in clockwise direction) is equal to $\pi/3$ and on the third to $2\pi/3$.

(b) Each charged plaquette has three nearest neighbor plaquettes. Two of these have another charged plaquette

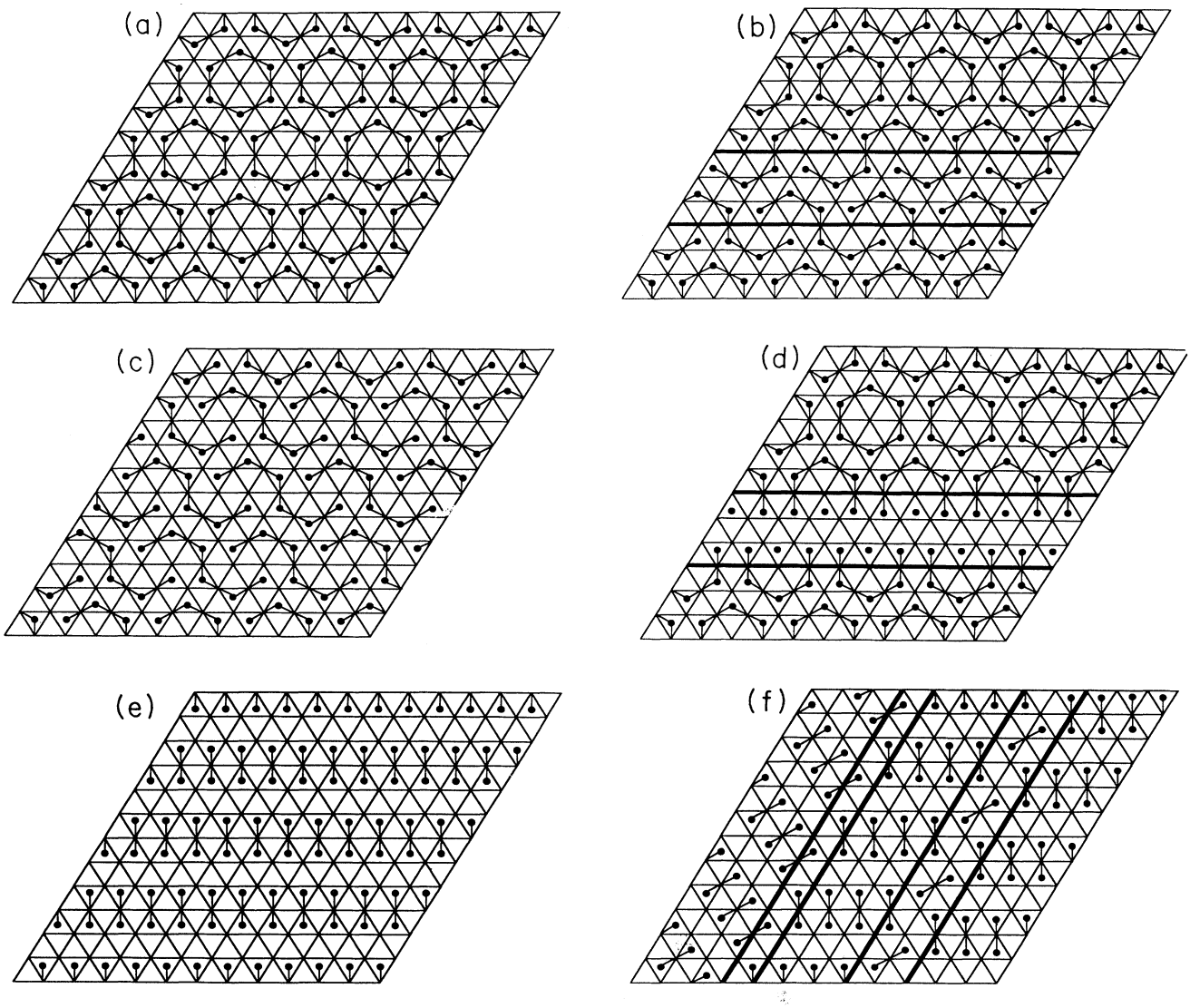

FIG. 2. $f=1/3$. (a) Hexagonal ground state. The $\phi_{\mathbf{r}\mathbf{r}'}$'s can be determined by the rules given in the text: the bonds carrying the value $2\pi/3$ form hexagons containing six noncharged plaquettes. The $\phi_{\mathbf{r}\mathbf{r}'}=0$ lines form a triangular sublattice the nodes of which are the centers of the hexagons. The partial discrete degeneracy of this ground state due to the lattice symmetry equals 9. (b) Ground state with two parallel zero energy domain walls along $\phi_{\mathbf{r}\mathbf{r}'}=0$ lines with different signs of the translation vector. The same hexagonal ground state lies above and below the zero energy defect. (c) Necklace ground state obtained from the hexagonal one with zero energy domain walls with the smallest possible distance and each one with the same sign for the corresponding translation vector. (d) Ground state with a strip consisting of a different configuration. As the horizontal $\phi_{\mathbf{r}\mathbf{r}'}=0$ lines are still there, it is still possible to perform shifts along them. Therefore we could also consider this strip as a thick zero energy domain wall. (e) Linear ground state obtained by repetition of the thick zero energy domain wall of (d). (f) Different linear ground states separated by zero energy domain walls not corresponding to $\phi_{\mathbf{r}\mathbf{r}'}=0$ lines. (g) Butterfly ground state obtained by a repetition of the wall depicted on the right hand side of (f). (h) Ground state with infinite size zero energy domain walls crossing one another. The horizontal domain walls correspond to those of (c). The vertical one corresponds to (d) but has been broken by the horizontal ones.

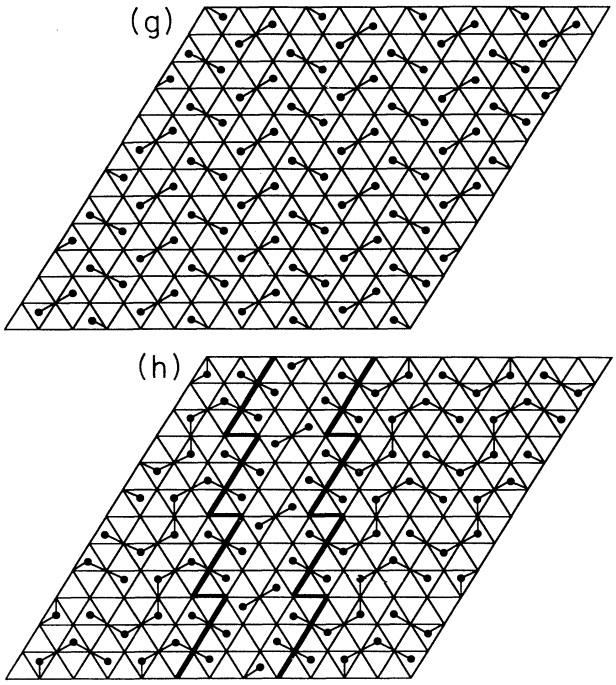

FIG. 2 *(Continued).*

as nearest neighbor, whereas the third does not. $\phi_{\mathbf{r}\mathbf{r}'}$ is equal to $2\pi/3$ on the bond which is ajacent to this particular plaquette.

(c) The bonds lying between uncharged plaquettes carry a zero value of ϕ.

The hexagonal ground state of the $f=1/3$ model allows also for the construction of zero energy domain walls with more complex structure [Fig. 2(d)]. Placing such strips one after another it is possible to construct the ground state with linear structure [Fig. 2(e)] that looks quite different from the hexagonal one. Of course different combinations of parallel strips of hexagonal, necklace, and linear ground states are also possible.

On the background of the linear ground state the zero energy domain walls can be constructed which are not related to $\phi_{\mathbf{r}\mathbf{r}'}=0$ lines [Fig. 2(f)]. Repeating such walls one after the other it is possible to construct one more periodic ground state ["butterfly" ground state, Fig. 2(g)] that again differs very much from all the states considered before. It is interesting to note that we have three different regular ground states (hexagonal, linear, and butterfly) which represent three different groups of planar symmetries.

It is also possible to construct ground states with infinite size zero energy domain walls crossing one another [Fig. 2(h)]. Indeed linear strips as in Fig. 2(d) in one direction and shifts as in Fig. 2(c) in another can be combined without change of energy. The example of Fig. 2(h) could be extended from the top of the figure by a hexagonal ground state with a nonbroken linear strip [as in Fig. 2(d) but with the strip in a different direction]. So there are many possible combinations, but the linear strips cannot be accompanied by any additional shift in the same direction and the shifts have to correspond to the same sign of the translation vector [as in Fig. 2(c)]. It is possible that other zero energy domain walls may exist. However, we have never found a ground state with zero energy defects of finite size.

B. Spin-wave free energy

We have calculated the spin-wave free energy for four different periodic ground states: hexagonal, necklace, linear, and butterfly. The coefficient μ in Eq. (9) is reported in Table II. As in the case of $f=1/4$ the hexagonal ground state (which, by the way, has the highest symmetry) turns out to have the lowest spin-wave free energy. This means that at low but finite temperatures this state will be dominant and the zero energy domain walls on its background will have a small but positive free energy.

As in the case of $f=1/4$ the extended defects with the lowest free energy have the form of strips enclosed by zero energy domain walls with finite energy defect end points. But now, starting from the hexagonal ground state, we can make such a defect not only by shifting the charges in the strip, but also by deplacing them to obtain the linear ground state inside the strip. We report in Table III the coefficient μ associated with periodic ground states constructed with a succession of such strips of infinite length. First we compare the hexagonal ground state with three different concentrations ν of domain walls: $\nu=0$ (corresponding to the hexagonal state), $\nu=1/6$ (corresponding to a shift on every sixth line), and $\nu=1/3$ (shift on every third line, which is the closest possible spacing). There are two results for $\nu=1/3$: The first (a) corresponds to the necklace state and the second (b) to shifts with regularly alternating directions [as in Fig. 2(b) but with a periodicity corresponding to six consecutive horizontal lines]. Finally, the two last results of Table III represent strips of the linear state (with periodicity corresponding to twice the strip width): The first corresponds to Fig. 2(d) and the second to a strip with the same hexagonal ground state below and above each strip [which is not the case in Fig. 2(d)].

From these results we conclude that the free energy associated with a $\phi_{\mathbf{r}\mathbf{r}'}=0$ domain wall separating two different hexagonal ground states is equal to $\gamma T \approx 6.3\times10^{-2}T$ per unit length. This gives $\alpha_s = 2\gamma \approx 0.125$ for the coefficient for a strip constructed by shifting. We will call such a strip a "shifted strip defect." We assume that the free energy will also be proportional to the concentration of strips of linear ground state. Thus we can ascribe a

TABLE II. $f=1/3$. Coefficient μ of the spin-wave free energy for four different types of ground state (g.s.)

g.s. type	μ	$\Delta\mu \equiv \mu - \mu(0)$
Hexagonal	0.23647	0
Necklace	0.25720	2.073×10^{-2}
Linear	0.26840	3.193×10^{-2}
Butterfly	0.33321	9.674×10^{-2}

TABLE III. f=1/3. ν is the fraction of the number of lines (in one direction) with a zero energy domain wall. This table shows the linearity of the spin-wave free energy as a function of the number of zero energy domain wall. The first value for ν=1/3 corresponds to shifts in the same direction and with the same orientation of the corresponding translation vectors, and the second to shifts with alternating opposite orientations. The two last lines correspond to periodic ground states with one linear strip every six lines. The second of them corresponds to an additional shift between the configuration of charge below and above the linear strip.

g.s. type	μ	$\Delta\mu$	γ
ν =0	0.23647	0	–
ν =1/6	0.24709	1.062×10^{-2}	6.372×10^{-2}
(a) ν =1/3	0.25720	2.073×10^{-2}	6.219×10^{-2}
(b) ν =1/3	0.25742	2.095×10^{-2}	6.285×10^{-2}
Linear strip	0.26607	2.960×10^{-2}	–
Linear strip+shift	0.26562	2.915×10^{-2}	–

value $\alpha_l = 6\Delta\mu \approx 0.18$ to the coefficient giving the free energy per length of a strip of linear ground state (the factor of 6 comes from the fact that there is one strip per six horizontal lines). We will call such a strip a linear strip defect. Comparing the two last results of Table III with the case of the uniform linear ground state in Table II we can decompose the free energy of a linear strip into two terms. The first of them can be associated with the "bulk" free energy of the linear state inside the strip and the second can be related to the boundaries between the two types of ground states.

C. Low-temperature defects and phase transitions

In contrast with the case of f=1/4 we now have to consider two kinds of extended defects at low temperature: the shifted strip defects [Fig. 2(b)] and the linear strip defects [Fig. 2(d)]. So we can calculate (numerically) the energies of the end points of each defect and estimate the characteristic temperatures in the same way as was done in Sec. III C but using a value of m equal to 4.5 (now the width of the strips is equal to 3 and their length can only be a multiple of 3/2). The results are shown in Table IV. We obtain that the characteristic temperature T_{*l} related to the linear strip defects is lower than T_{*s} related to the shifted strip defects. Thus although the lowest spin-wave free energy is for the defect of shifting type, the linear defects will be more numerous because of their lower defect end point energy.

TABLE IV. f=1/3. Characteristics of the two kinds of strip defects appearing at low temperature. The concentration c is calculated with Eq. (14). It can be noted that although α is not so small the approximation ($\alpha \ll 1$) we use to produce the definition of T_* [Eq. (17)] is not relevant according to the number of digits that are shown.

Defect	α	E_0	$\langle L\rangle$	T_*	$c(T=0.03)$	$c(T=0.1)$
Shift. strip	0.125	0.18	9	0.06	0.31×10^{-4}	0.12
Linear strip	0.18	0.086	6.5	0.03	1.08×10^{-2}	0.38

Nonetheless, the phase transition related to the disappearance of the discrete ordering should be associated with agglomeration and merging of shifted strip defects because only proliferation of these defects is equivalent to intermixing of different hexagonal states while linear strip defects correspond to the appearance of metastable states of the other type (involving an additional bulk free energy). Therefore we should use T_{*s} and not T_{*l} as an estimate for the transition temperature although such estimate would be less certain than for $f = 1/4$ due to the presence of the strip defects of the other type.

But as for f=1/4 we can still expect the hexagonal order to be destroyed at a logarithmically small temperature. It can be noted that the estimated temperatures are lower than for f=1/4 because of the lower defect end point energy. But even if the values of α are not so small, it is the zero energy domain walls that are responsible for the peculiar behavior leading to a temperature decrease of the phase transitions.

So the discussion of the different scenarios of the phase transitions that was made for f=1/4 in Sec. III C is also applicable for f=1/3. However, there may be two relevant differences between the two cases. First of all, the helicity modulus is likely to be more affected (at $T \sim T_{*s}$) due to the two kinds of low-temperature defects and thus the transitions may appear in a different sequence. Second, the type of discrete degeneracy associated with the hexagonal ground state is not the same for both cases; thus the transitions may be of a different nature.

Thus for both values of frustrations, the hexagonal order is destroyed at an unusually low temperature that depends on the spin-wave free energy of the zero energy domain walls. The latter are, furthermore, responsible for the lower temperature of the drop of the helicity modulus.

It is interesting to note that in contrast to the case of f=1/4, in the f =1/3 model the accidental degeneracy of the ground states will be removed if the form of the interaction is changed; that is, the higher harmonics are added to the interaction in Eq. (1). For example, in the superconducting wire network the effective interaction function at low temperature is very close to a piecewise parabolic function (with a periodicity of 2π). In that case the butterfly ground state of Fig. 2(g) will have the lowest energy. For $f = 1/4$ the accidental degeneracy cannot be removed by such a change of interactions.

V. MONTE CARLO SIMULATIONS

In this section we discuss some snapshots we have taken during Monte Carlo simulations and compare our predictions with what has been seen in simulations made by the other authors.

The striking feature of our shots (each from a 36×36 site system) is the disappearence of the hexagonal ordering at temperatures close to our estimates of T_* [cf. Figs. 3(a) and 3(c)]. Furthermore, the structure of the defects appearing at low temperature corresponds well to our analysis. In particular for f=1/3 at T=0.03 ($\approx T_{*l}$)

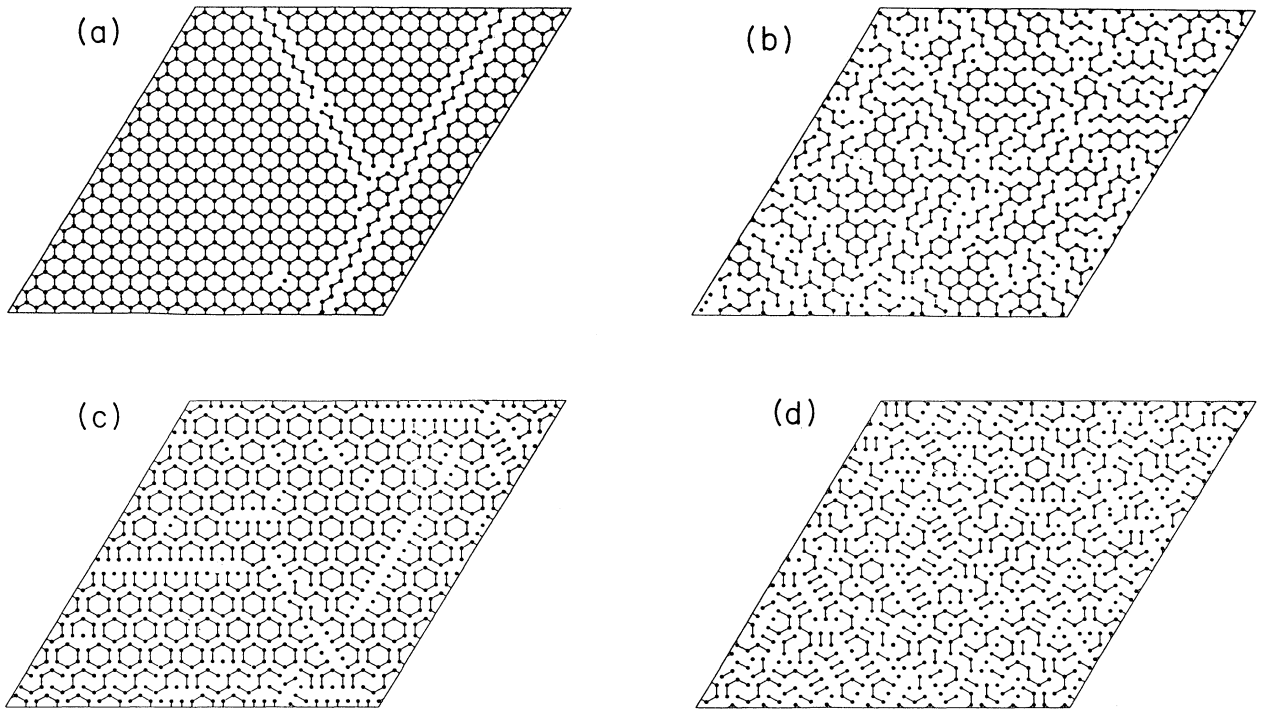

FIG. 3. $f=1/4$. (a) Snapshot at $T=0.1$ close to T_*. The segments linking the charges are a guide to the eye. We can spot two long defects. One of them runs through the whole lattice. The concentration c calculated with Eq. (14) is equal to 0.44×10^{-2}. (b) $f=1/4$. Snapshot at $T=0.25$ greater than T_*. The strip defects have broadened and we are not able to define clearly a main representative among the four hexagonal ground states. The concentration c calculated with Eq. (14) is equal to 0.46. (c) $f=1/3$. Snapshot at $T=0.03$ close to T_{*l}. We can mainly observe the presence of linear strip defects. Two shifted defects also occur but they are continued by linear ones which are likely to weaken the energy of their end points. (d) $f=1/3$. Snapshot at $T=0.1$ slightly greater than T_{*s}. Numerous defects are present and the hexagonal order is lost. We can also observe the rare occurrence of the butterfly ground state that would involve a higher spin-wave free energy.

mainly linear defects can be seen [Fig. 3(c)], whereas at $T=0.1$ both kinds of defects are present, although they cannot easily be distinguished because of their high density [cf. Fig. 3(d)].

Although the concentration c evaluated using Eq. (14) and quoted in the figure captions for $f=1/4$ and in Table IV for $f=1/3$ corresponds well to the shots observed close to T_* for both values of f, it is overestimated for higher T because the short-range interaction between the defects has not been taken into account. Obviously, the average length of the defects is equally overevaluated because we neglect the influence of the crossing energy of the defects. For $f=1/4$ we have found numerically that the crossing energy is twice the defect end point energy. For $f=1/3$, it depends on the particular type of defect crossing.

However, in several shots taken at low temperatures we have seen a strip defect going through the whole lattice [cf. Fig. 3(a)]. Such a defect has an abnormally low energy because of the lack of defect end points. This is a finite size effect that could deeply perturb the behavior of the system in the numerical simulations. Indeed such a defect has no energy dependence on the strip width (note that this is not true for the linear strip defect for $f=1/3$). So if the system size is not much larger than the typical size of the defects, the abnormal defect could take on too much statistical importance.

Finally, for both values of frustrations the hexagonal order seems clearly destroyed on the shots corresponding to a temperature larger than T_* in agreement with our predictions [see Fig. 3(b) for $f=1/4$ at $T = 0.25$, and see Fig. 3(d) for $f=1/3$ at $T=0.1$].

The Monte Carlo simulations on the triangular lattice made by Shih and Stroud[3] and by Kim, Lee, and Choi[9] (up to sizes of 256×256 for $f=1/4$) indicate that the phase transitions occur at an unusually low temperature for the frustrations $f=1/4$ and $f=1/3$. These temperatures correspond well to our analysis. Indeed for $f=1/4$ a maximum of the specific heat has been observed at $T \sim 0.15$ and this corresponds to the temperature of the proliferation of kinks we have estimated. The helicity modulus observed at this temperature seems to be larger than its critical value, but this is not conclusive because strong finite size effects are also observed even in large systems. Anyway, it drops at lower temperature than in any studied frustrated XY model without accidental de-

generacy. As for $f=1/3$, the helicity modulus drops at a temperature even lower than for $f=1/4$; this is as well in accordance with our conclusions.

Quite generally, it is rather difficult to study numerically the nature of the phase transitions in the XY model with accidental degeneracy because system sizes much larger than the typical size of the strip defect are needed to observe the destruction of the discrete ordering and still larger scales would be involved if one is interested in investigation of the mutual influence of two types of disordering. Therefore it may be rather difficult even to distinguish whether one single or two separate transitions take place.

VI. CONCLUSION

We have investigated the XY model on the triangular lattice for $f=1/4$ and $f=1/3$. Both values of the frustration manifest an infinite discrete degeneracy and a wide variety of the ground states which are related to each other not by the symmetries of the lattice but by the possibility of the construction of the special zero energy domain walls. This feature is the cause of the unexpected behavior which has been seen in numerical simulations.

At an arbitrarily small temperature the infinite degeneracy is removed by the spin-wave free energy, and in both cases studied the most favorable state is the one with the hexagonal symmetry (which is the highest degree of symmetry possible). The low free energy of the spin waves results in the unusual anisotropic form of the typical defects at low temperatures. Our low-temperature analysis allows us both to understand what low-temperature defects should be observed in numerical simulations and to obtain an estimate for the characteristic temperature below which nothing relevant should happen. At slightly higher temperature, but still small in comparison with critical temperatures for the other values of frustration (of the form $f=p/q$ with some small q) devoid of zero energy domain walls, both the hexagonal order associated with the discrete degeneracy of the hexagonal ground state and the XY quasi-long-range order are likely to be destroyed. However, we cannot draw any precise conclusions about the nature of the phase transitions. We have discussed various scenarios for the temperature behavior and pointed out some differences between $f=1/4$ and $f=1/3$ which could be relevant for the phase transitions of these systems.

Our analysis is supported by the results of Monte Carlo simulations. In the experimental situation the implications of the accidental degeneracy could be more difficult to observe because the details of the particular system can be important. As an example, the accidental degeneracy of the ground state can be removed by a small difference of the form of the phase-phase interaction (as happens for $f = 1/3$). Nevertheless, even if this degeneracy is removed, it is likely that an abnormal number of metastable states with low energy will persist, which could again be responsible for more numerous low-temperature excitations being possibly less mobile than other defects, since (around the critical temperatures) they would imply a more complex structure than usual. So it seems possible that a peculiar frequency behavior might be seen in dynamical measurements[10] on superconducting networks and arrays corresponding to an XY model with accidental degeneracy.

ACKNOWLEDGMENT

This work was supported by the Swiss National Science Foundation.

[1] For a review see *Proceedings of the NATO Advanced Research Workshop, Delft, 1987*, edited by J. E. Mooij and G. B. E. Schön [Physica B **152**, 1 (1988)].

[2] J. Villain, J. Phys C **10**, 4793 (1977); D. H. Lee, J. D. Joannopoulos, J. W. Negele, and D. P. Landau, Phys. Rev. Lett. **52**, 433 (1984).

[3] W. Y. Shih and D. Stroud, Phys. Rev. B **30**, 6774 (1984).

[4] M. Y. Choi and S. Doniach, Phys. Rev. B **31**, 4516 (1985).

[5] W. Y. Shih and D. Stroud, Phys. Rev. B **32**, 158 (1985).

[6] S. E. Korshunov, J. Stat. Phys. **43**, 17 (1986).

[7] R. K. Brown and J. C. Garland, Phys. Rev. B **33**, 7827 (1986); R. Théron, J. B. Simond, J. L. Gavilano, Ch. Leemann, and P. Martinoli, Physica B **165**, 1641 (1990); R. Théron, S. E. Korshunov, J. B. Simond, Ch. Leemann, and P. Martinoli, Phys. Rev. Lett. **72**, 562 (1994).

[8] H. Kawamura, J. Phys. Soc. Jpn. **53**, 2452 (1984); S. E. Korshunov, J. Phys. C **19**, 5927 (1986); C. L. Henley, J. Appl. Phys. **61**, 3962 (1987).

[9] S. Kim, S. Lee, and M. Y. Choi, Phys. Rev. B **46**, 1240 (1992).

[10] P. Martinoli, Ph. Lerch, Ch. Leemann, and H. Beck, Jpn. J. Appl. Phys. **26**, Suppl. 26-3, 1999 (1987); R. Théron, J. B. Simond, Ch. Leemann, H. Beck, P. Martinoli, and P. Minnhagen, Phys. Rev. Lett. **71**, 1246 (1993).